

# MACROSCOPIC WORKLOAD MODEL FOR ESTIMATING EN ROUTE SECTOR CAPACITY

*Jerry D. Welch, John W. Andrews, and Brian D. Martin*

*M.I.T. Lincoln Laboratory, Lexington, MA 02420-9185*

*Banavar Sridhar*

*NASA Ames Research Center, Moffett Field, CA 90435*

## Abstract

Under ideal weather conditions, each en route sector in an air traffic management (ATM) system has a certain maximum operational traffic density that its controller team can safely handle with nominal traffic flow. We call this the *design* capacity of the sector. Bad weather and altered flow often reduce sector capacity by increasing controller workload. We refer to sector capacity that is reduced by such conditions as *dynamic* capacity.

When operational conditions cause workload to exceed the capability of a sector's controllers, air traffic managers can respond either by reducing demand or by increasing design capacity. Reducing demand can increase aircraft operating costs and impose delays. Increasing design capacity is usually accomplished by assigning more control resources to the airspace. This increases the cost of ATM.

To ensure full utilization of the dynamic capacity and efficient use of the workforce, it is important to accurately characterize the capacity of each sector. Airspace designers often estimate sector capacity using microscopic workload simulations that model each task imposed by each aircraft. However, the complexities of those detailed models limit their real-time operational use, particularly in situations in which sector volumes or flow directions must adapt to changing conditions.

To represent design capacity operationally in the United States, traffic flow managers define an acceptable peak traffic count for each sector based on practical experience. These subjective thresholds—while usable in decision-making—do not always reflect the complexity and geometry of the sectors, nor the direction of the traffic flow.

We have developed a general macroscopic workload model to quantify the workload impact of traffic density, sector geometry, flow direction, and air-to-air conflict rates. This model provides an objective basis for estimating design capacity.

Unlike simulation models, this analytical approach easily extrapolates to new conditions and allows parameter validation by fitting to observed sector traffic counts. The model quantifies coordination and conflict workload as well as observed relationships between sector volume and controller efficiency.

The model can support real-time prediction of changes in design capacity when traffic is diverted from nominal routes. It can be used to estimate residual airspace capacity when weather partially blocks a sector. Its ability to identify dominant manual workload factors can also help define the benefits and effectiveness of alternative concepts for automating labor-intensive tasks.

## Introduction

We define the design capacity of a sector as the maximum operational traffic density that a controller team can safely handle in clear weather with nominal traffic flow. We have extended an existing macroscopic workload model to estimate sector design capacity. The result is an analytical model that quantifies the workload impact of sector geometry, flow direction, and air-to-air conflicts. Unlike simulation models, this analytical approach easily extrapolates to a range of conditions.

The capacity of an en route air traffic sector is limited more by controller workload than by aircraft separation standards. The capacity of a volume of en route airspace based solely on international separation standards is much larger than the design capacity of an air traffic control sector of the same volume [1, 2, 3].

Bad weather, altered flow patterns, and other conditions can increase controller workload and reduce capacity below its design value. The resulting reduced capacity is the dynamic capacity of the sector, and by analogy a weighted combination of traffic density and other controller workload determinants is sometimes referred to as “dynamic density” [4].

When dynamic density grows such that workload exceeds the capability of the controller team assigned to a sector, air traffic managers can either reduce traffic demand or reconfigure the system to increase the design capacity of the airspace. Reducing demand tends to increase aircraft operating costs and impose delay. Reconfiguring to increase capacity tends to reduce air traffic management efficiency by employing more controller resources per aircraft. The most common operational means of increasing design capacity in today's manual system is to partition a sector into two smaller sectors, each with an independent controller team.

A number of studies have addressed the process of quantifying the air traffic management complexity factors that influence controller workload [5, 6, 7]. Others have demonstrated the feasibility of predicting future workload changes based on extrapolation of flight plan and trajectory data [8, 9]. Research is also under way to quantify and forecast the effects of hazardous weather on airspace capacity [10]. Weather can reduce capacity in two ways. It can simply reduce the available volume of safe airspace in a sector, or it can increase control complexity. A focus of current weather capacity research has been on predicting airspace blockage [11].

To represent the design capacity of en route sectors in today's operational conditions, traffic flow managers currently define instantaneous aircraft count thresholds based on operational experience. While usable in the context of overall decision-making, these subjective "monitor alert" thresholds cannot be extrapolated to dynamic situations because they do not always accurately reflect actual sector characteristics. (High aircraft count thresholds are sometimes assigned to small sectors, even though the resulting aircraft density would become unmanageable if the count were to approach the assigned number.)

Airspace designers often employ microscopic workload simulations to estimate sector capacity [12]. These simulations account for every task imposed by a specific set of individual aircraft and flow conditions. The complexities of those detailed models limit their use as tactical tools in situations where flow conditions can change in real time or in which airspace boundaries may adapt dynamically to changing conditions.

Unlike simulation models, an analytical model can be quickly extrapolated to a wide range of conditions. Extrapolation also allows one to validate the model's parameters by fitting its capacity predictions to peak traffic observations for large numbers of sectors. The

model quantifies the magnitude of coordination and conflict workload and explains observed operational relationships between sector volume and controller efficiency.

This model has important potential operational applications. It could support real-time estimation of changes in design capacity when traffic must divert from nominal routes and it could allow real-time estimation of residual airspace capacity when weather partially blocks a sector.

Because the model separately quantifies coordination and conflict workload intensity, it can help define the benefits and effectiveness of proposed future air traffic management automation concepts such as those of the Next Generation Air Traffic System (NGATS). NGATS is expected to allow more dynamic use of routes and airspace, and to apply automation to the reduction of workload. As the NGATS program prioritizes its research efforts, it will be essential to understand which types of workload dominate in particular situations.

### ***Task-based Workload Models***

Many of the attributes of a sector and its traffic can be expressed in terms of the ways those attributes generate tasks for the controller. If there are J distinct tasks, we could express the workload metric as

$$G = \sum_{j=1}^J \tau_j \lambda_j.$$

Here  $\tau_j$  is the time required to complete task j, and  $\lambda_j$  is the rate of its occurrence. The model provides a physical starting point by viewing the tasks as distinct segments of the timeline. The metric G can then be considered "workload intensity" or the fraction of the available time in which a sector controller is busy executing tasks. There is a certain value  $G_m$  at which a controller will feel uncomfortable accepting additional traffic. This maximum comfort level defines the capacity of the sector.

Detailed simulation models, such as Eurocontrol's Reorganized ATC Mathematical Model Simulator (RAMS) [12], MITRE's Collaborative Routing Coordination Tool (CRCT) [13], or NASA's Center/TRACON Automation System (CTAS) [14] define multiple distinct tasks, each with its unique weighting time. Such microscopic models can, in principle, provide rich insight into sector design considerations and the sources of workload. However, their results are difficult to validate and

interpret. A proliferation of task types requires regression to generate clear relationships for operational use. One can simplify modeling and validation by aggregating all the distinct tasks into only a few general types [15, 16]. This macroscopic approach provides less detailed information, but is appropriate for examining broader design and operational issues. Aggregating the tasks also makes it easier to determine model parameters using experimental or operational data. We estimate most occurrence rates from the known characteristics of the airspace and traffic. This leaves only a small set of unknown task times to be determined by fitting the model to peak sector traffic throughput observations.

## Components of the Workload Model

Our aggregated model employs four task types, differentiated according to their occurrence characteristics. Most defined controller activities can be uniquely and unambiguously assigned to one of the four task types.

The four task types are defined as *background*, *transition*, *recurring*, and *conflict* tasks.

*Background* tasks occur without respect to the number of aircraft in the sector. We consider them to occur at a mean rate  $\lambda_b$  and to require a mean time  $\tau_b$  to complete. Background tasks include routine activities such as configuring displays, coordinating with managers and supervisors, maintaining work areas, verifying surveillance performance, and examining weather forecasts. These tasks absorb a small constant fraction of controller time  $G_b = \tau_b \lambda_b$ .

*Transition* tasks occur each time an aircraft passes through the sector. They include tasks such as hand-off acceptance, initial contact, familiarization with flight plan information, and initial route planning. We aggregate transition tasks by considering them to require a mean time  $\tau_t$  to complete and to occur at a mean rate  $\lambda_t$ . The occurrence rate of transition tasks is equal to the average number of aircraft in the sector  $E[N]$ , divided by the average transit time through the sector  $T$ . This rate is thus equivalent to the sector throughput:

$$\lambda_t = E[N]/T.$$

*Recurring* tasks occur repeatedly while each aircraft remains in the sector. These tasks can also be aggregated to require a mean time  $\tau_r$  to complete. They recur at a mean rate  $\lambda_r$ , where

$$\lambda_r = E[N]/P.$$

Here  $P$  is the mean task recurrence period per aircraft. Recurring tasks include activities such as traffic scanning, restricted airspace and hazardous weather avoidance, flight plan changes, and status updates. Recurring tasks also include activities meant to prevent conflicts, such as conformance monitoring and separation planning.

*Conflict* tasks occur when there are conflicts between two aircraft. (Although conflicts between three or more aircraft are of major concern to controllers, this concern is usually triggered by a pair-wise conflict. The multi-aircraft conflict *rate* is too small relative to the pair-wise conflict rate to require separate handling.) Conflict tasks include such activities as conflict detection, vectoring for conflict resolution, consideration of secondary encounters, and post-conflict route recovery. We aggregate conflict tasks by considering them to require a mean time  $\tau_c$  to complete and to occur at a mean rate  $\lambda_c$ . For a sector with a particular aircraft count  $N_s$ , the conflict rate varies as the square of  $N_s$  divided by the sector volume  $Q$ .

$$\lambda_c = BN_s^2/Q.$$

In this equation  $B$  is a physical constant based on aircraft closing speeds and separation standards [17]:

$$B = 2M_h M_v E[V_{12}],$$

where  $M_h$  and  $M_v$  are the horizontal and vertical miss distances that define a separation violation, and  $E[V_{12}]$  is the expected value of the closing speed.

In general, the sector traffic count  $N$  is a random variable [18], and  $\lambda_c$  is proportional to the expected value  $E[N^2]$ . If  $N$  is Poisson distributed, the variance and mean of  $N$  are identical, and

$$E[N^2] = (E[N])^2 + E[N].$$

If the local volumetric traffic density is  $\kappa$ , then

$$\kappa Q = E[N].$$

The Poisson assumption gives a mean conflict rate

$$\lambda_c = B\kappa(\kappa Q + 1).$$

## Total Workload Intensity

The total workload intensity  $G$  is the fraction of the controller's available time devoted to all four of these task types:

$$G = \tau_b \lambda_b + \tau_t \lambda_t + \tau_r \lambda_r + \tau_c \lambda_c.$$

This expands to:

$$G = G_b + \tau_t \kappa Q / T + \tau_r \kappa Q / P + \tau_c B\kappa(\kappa Q + 1).$$

We compute the rate-related terms ( $\kappa$ ,  $T$ ,  $B$ , and  $Q$ ) directly from sector geometry and traffic parameters. The values ( $G_b$ ,  $\tau_t$ ,  $\tau_r$ ,  $P$ , and  $\tau_c$ ) are all empirical. Some work time values have been measured in prior modeling efforts: ( $\tau_c$  and  $\tau_t$ ) [16], and ( $\tau_r$ ) [12]. We have determined the remaining model parameters by adjusting them to fit the model's capacity predictions to peak sector traffic observations. This regression process is explained below.

Figure 1 illustrates sample workload results based on our estimated and fitted model parameters for a typical 10,000 cubic nautical mile ( $\text{nm}^3$ ) sector with a floor-to-ceiling height of 10,000 ft. The parameters in the figure legend are all defined above. The mean encounter closing speed of 440 kt is based on an assumption of two opposing traffic streams with randomly located aircraft all flying at a common speed of 550 kt, with 72% of the aircraft flying in one direction and 28% in the other.

The graph shows the four individual workload intensity components as a function of aircraft count. The sum of background, transition, recurring, and conflict tasks reaches a nominal  $G_m$  comfort limit of 80% when the sector traffic count reaches 16 (a density of 16 aircraft per 10,000  $\text{nm}^3$ ). A count of 16 aircraft is typical of the observed peak instantaneous traffic count for an en route sector of that volume in US airspace. When this sector operates near capacity, conflict workload is the largest workload component. This information can help focus and prioritize activities intended to automate the air traffic management process.

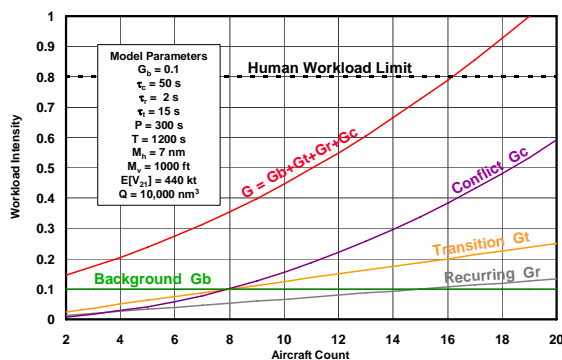


Figure 1. Model workload intensity vs. aircraft count for a sector volume of 10,000  $\text{nm}^3$ .

## Determining the Model Parameters

The four-component model is an extension of an early model by Schmidt [15, 16], which was used by the FAA Technical Center to predict sector staffing and console requirements resulting from anticipated en route traffic growth. Schmidt's workload

simulations suggested a mean  $\tau_c$  of 55s of aggregated activity for each conflict event and a transition  $\tau_t$  ranging from 28s to 46s depending on sector type. His simulation experiments also indicated that when  $G$  equaled 80% of the total time available, controllers reported that the sector had reached its maximum loading  $G_m$ . (Others [12] consider  $G_m$  to be closer to 0.7.)

The original Schmidt model did not include a general means of estimating conflict rates, nor did it distinguish recurring tasks from transition tasks. We previously extended the model [17] to allow direct computation of conflict rates based on assumptions of unstructured flow and Poisson-distributed arrivals.

We have now added recurring tasks to allow us to study the relationship of workload to sector size. Understanding this relationship is important when validating the model parameters based on measured sector traffic data.

It is not possible to uniquely determine empirical model parameters that fit all sector workload conditions. Some important practical conditions that can increase workload are not explicitly addressed by the model. We address the more constrained problem of determining the traffic count bound  $N_m$  that causes workload to equal the intensity limit  $G_m$  under ideal conditions. Using parameters and traffic flow assumptions that minimize workload, we set the expression for workload intensity  $G$  equal to  $G_m$ , and invert the quadratic equation to solve for the design capacity  $N_m$ .

## Analytical Relationship between Design Capacity and Sector Volume

For a region of constant airspace density, the recurring and conflict workload components depend directly on sector volume. The transition workload component is proportional to the sector volume and is inversely proportional to the mean transit time through the sector. Transit time depends on the length of the sector. In fact, en route sectors are often elongated in the direction of predominant traffic flow with the express purpose of reducing the transition workload component. We exploit this fact to derive an informative approximation of the design capacity of a sector directly from its volume and shape.

In a set of sectors of the same floor-to-ceiling height, we can relate the longest sector dimension to the sector volume by assuming a two-dimensional rectangular shape. Many high-capacity sectors approximate rectangles, sometimes elongated by length/width ratios as great as four to one. If we assume that all sectors are rectangular, have known

lengths, and that flow is entirely longitudinal, we can calculate a sector's capacity directly from its volume and its length-to-width ratio. For a given volume, square sectors have less capacity, and elongated sectors have greater capacity, but the general dependence on volume is identical.

Figure 2 illustrates the relationship between design capacity  $N_m$  and sector volume for the same set of model parameters used in Figure 1, except that here the transit time  $T$  varies with sector volume. The figure is based on 10,000 ft high rectangular sectors and plots design capacity separately for three rectangular length-to-width ratios, 1:1 (square), 2:1, and 4:1. For a sector volume of 10,000  $\text{nm}^3$ , the modeled design capacity increases from about 13 aircraft for a square sector to about 16 aircraft for a sector with a 4:1 length-to-width ratio.

Capacity does not grow as fast as sector volume. Thus, for a sector operating at design capacity, the peak volumetric traffic density that the sector can handle decreases as the sector grows.

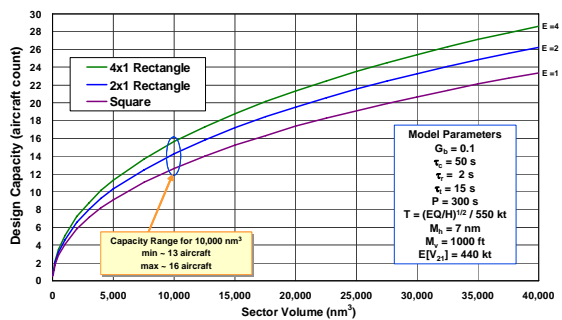


**Figure 2. Modeled design capacity for 10,000 ft high rectangular sectors with length-to-width ratios of 1:1 (square), 2:1, and 4:1.**

### Monitor Alert Thresholds

This non-linear dependence of capacity on volume is not reflected in current FAA traffic flow management sector overload thresholds. Figure 3 provides the ETMS Monitor Alert threshold values for a subset of en route sectors in the Northeastern United States where the Corridor Integrated Weather System (CIWS) has been implemented [19].

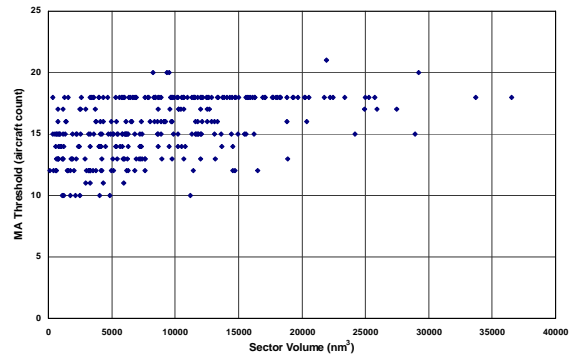


**Figure 3. ETMS Monitor Alert thresholds for CIWS sectors**

The threshold values are first-order invariant to sector volume. The most common thresholds are 15 or 16 aircraft per sector, and these values apply to sectors over the entire range of volumes. It will be shown below that a total of 16 aircraft in a small 1000  $\text{nm}^3$  sector would produce an aircraft density more than an order of magnitude larger than the mean density in the average size en route sector in the CIWS airspace. While this may be of little consequence in current traffic planning, it is clear that Monitor Alert thresholds are not reliable indicators of design capacity. They over-estimate the design capacity of small sectors and under-estimate design capacity in large sectors.

### Modeled Design Capacity for CIWS Sectors

Figure 4 plots the model's capacity estimate  $N_m$  for each of the sectors in the CIWS domain.

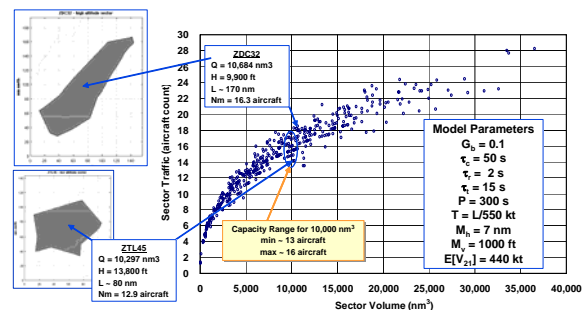


**Figure 4. Modeled design capacity of individual CIWS sectors.**

Variations in sector geometry are responsible for the observed variation in modeled values for sectors of similar volume. For example, the model capacities vary from 13 to 16 aircraft for those sectors that have volumes of approximately 10,000  $\text{nm}^3$ . The figure shows the shapes of two of those sectors in plan views drawn to a common scale. The elongated high-altitude sector ZDC32 ( $Q = 10,684 \text{ nm}^3$ ,  $H =$

9,900 ft,  $L \sim 170$  nm) has a modeled design capacity of 16.3 aircraft. The more nearly square low-altitude sector ZTL45 ( $Q = 10,297$  nm<sup>3</sup>,  $H = 13,800$  ft,  $L \sim 80$  nm) has a modeled design capacity of 12.9 aircraft.

## Comparing the Model with Peak Sector Traffic Measurements

Our approach to estimating actual design capacity is to directly analyze historical sector traffic in clear weather. We have measured traffic counts for all of the 455 CIWS en route sectors. To obtain peak traffic counts we average the number of aircraft in each sector for each 5-minute period during three clear-weather weekdays and select the period with the largest count. Most of the peak counts lie in a range between 6 and 14 aircraft (the average is 9 aircraft). Many of these counts are less than the design capacity because of insufficient traffic demand.

Figure 5 is a color-map of the peak observed traffic counts for the low en route sectors in the CIWS domain. An abnormally high 18-aircraft count occurred in the Toronto sector. This sector is unique among low sectors in that it extends from ground to 24,000 ft and includes Toronto's Pearson International Airport.

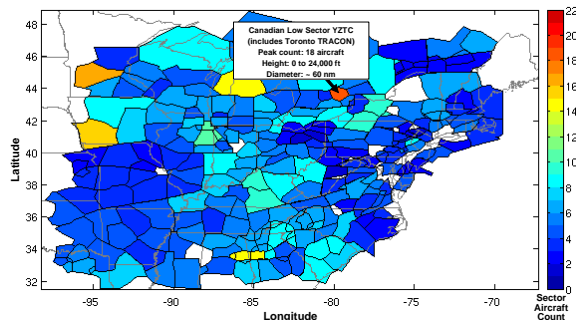


Figure 5. Peak clear-weather aircraft counts for CIWS low sectors.

Figure 6 maps the corresponding sector peak aircraft densities in aircraft per cubic nautical mile for the same low-altitude en route CIWS airspace.

There are a number of sectors of higher density than Toronto, mainly in the New York and Washington Centers. Although they have lower peak traffic counts than Toronto, they have higher densities because they have smaller heights.

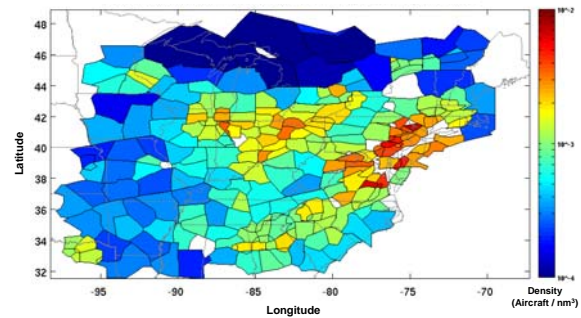


Figure 6. Peak clear-weather traffic densities (aircraft/nm<sup>3</sup>) for CIWS low sectors.

If the model is correct, the peak traffic count in a sector should not exceed the computed design capacity for that sector. To test this hypothesis, Figure 7 is a plot of traffic count versus sector volume which superimposes the observed peak traffic counts on the calculated capacities (From Figure 4, above) for all of the CIWS sectors.

Although most of the sectors operate at peak levels well below the modeled design capacity, the “frontier” trend for the maximum count at each volume is consistent with the model predictions in the sense that few sector counts exceed the bound. We intend to extend this analysis to other airspace regions to verify its generality.

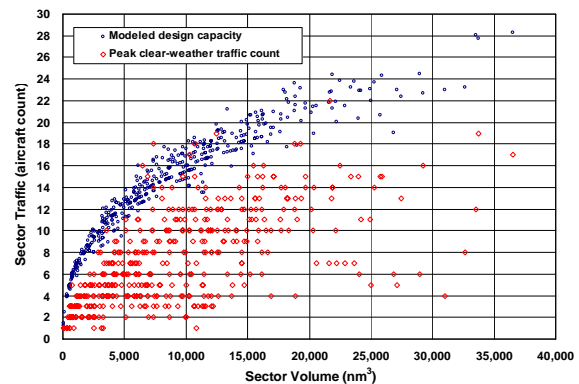
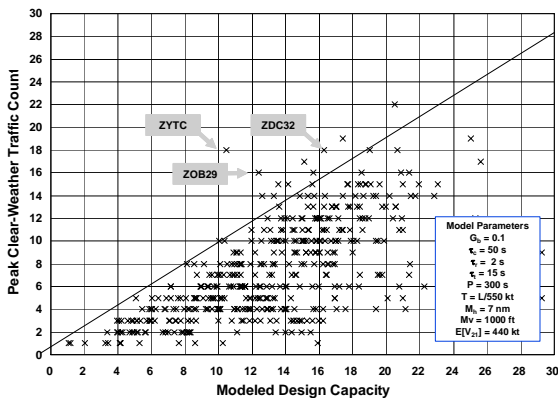


Figure 7. Peak traffic counts and modeled design capacity versus sector volume in CWIS airspace.

Complexity factors that are not explicitly related to sector volume can increase controller workload. For example, workload may increase when the sector experiences a high incidence of ascents and descents caused by proximity to airports. In principle, an increase in vertical rates could increase all three workload components. Altitude clearances could increase recurring workload. Transitions between higher and lower sectors could increase coordination workload. Increased trajectory uncertainty could increase conflict workload. The model allows one to adjust transit times and conflict thresholds on a

sector-by-sector basis to account for some of these effects.

The scatter-plot of Figure 8 shows the information from Figure 7 in a different way. Each point on this chart directly compares the peak clear-weather count and the modeled design capacity bound for a single sector.



**Figure 8. Peak counts vs. modeled design capacity for each en route sector in CIWS airspace.**

Only ten sectors have peak clear weather traffic counts that exceeded their model design capacity. Of these, only two had clear weather traffic counts that exceeded the design capacity bound by more than 2 aircraft. The three sectors flagged in the figure have high observed counts relative to their model predictions. The count of ZYTC, the Toronto TRACON, exceeds the modeled design capacity by 8 aircraft. The others are ZOB29, whose count exceeds the design capacity by 4 aircraft, and ZDC32 whose count exceeds the design capacity by 2 aircraft.

A number of geometric factors can affect sector capacity. The capacity model accounts for sector height as well as length and volume. Sector heights range from 1000 ft to more than 50,000 ft. If Toronto were a normal high sector with 60 mile diameter it would have a transit time of about 6 minutes. Its 24,000 ft height results in 12 minutes of vertical transit time if we estimate a mean vertical rate of 2000 ft/min. Its lateral transit time is also increased relative to other en route sectors because a significant fraction of its aircraft fly below 10,000 ft within 60 nm of the airport, and are thus limited to speeds below 250 kt. If we assume the mean ground speed in the sector is 300 kt, the mean lateral transit time is also 12 minutes (60 nm at 300 kt). A typical aircraft in this situation experiences nearly triple the nominal 6-minute transit time for level flight in a normal en route sector.

Another factor that can increase capacity relative to the model prediction is organized flow. The model's nominal conflict rate calculation provided earlier assumes a mean closing speed of 440 kt. If we reduce the encounter closing speed parameter in the model from 440 kt to 300 kt and triple the TORONTO transit time, ZYTC and ZOB29 are the only CIWS sectors with peak counts that exceed the model bound, and each has a calculated design capacity that is within 2 aircraft of the observed peak count.

### Traffic Density of En Route Sectors

Because design capacity does not increase in proportion to sector volume, large sectors cannot handle peak traffic densities as high as can small sectors. In fact, the principal means of accommodating local traffic density growth in today's manual system is to reduce the size of the local sectors. Although small sectors can handle high traffic densities, they are limited to small absolute aircraft counts. Sectors of all sizes require comparable controller teams when operating at maximum sector workload. Thus, small sectors experience lower productivity (peak aircraft handled per controller) than large sectors.

The decreasing traffic density capability of large sectors is evident in Figure 9, which plots the observed peak densities of the CIWS sectors as a function of volume. The solid line is the calculated achievable traffic density for a 10,000 ft high sector of rectangular cross section with 4:1 elongation. The highest observed traffic density occurred in the smallest sector, which is ZBW33 whose volume is  $58 \text{ nm}^3$ . Its peak count was one aircraft (resulting in a density of  $172 \text{ aircraft}/10,000 \text{ nm}^3$ ). This approaches an en route airspace traffic density defined solely by a 7-mile lateral and 0.2-mile vertical aircraft separation limit, which is one aircraft in a volume of approximately  $30 \text{ nm}^3$ . To provide additional context, the peak observed instantaneous traffic density of the entire CIWS high sector airspace volume was 749 aircraft in  $2,050,893 \text{ nm}^3$  or 1 aircraft in about  $2700 \text{ nm}^3$ . This is a relatively low air traffic density.

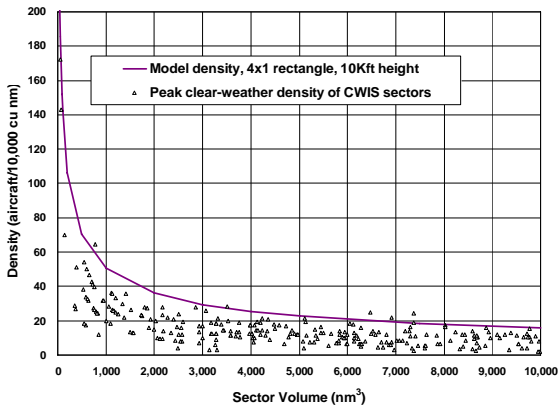


Figure 9. Traffic density of en route sectors.

### Variation of Modeled Workload Intensity Components with Volume

Figure 10 plots the model workload intensities of the conflict workload, transition workload, and recurring workload components as a function of sector volume for 4:1 rectangular sectors with optimal longitudinal flow when operating at capacity. (We omit background workload because it is invariant to sector volume.) All the model parameters are as in Figure 2.

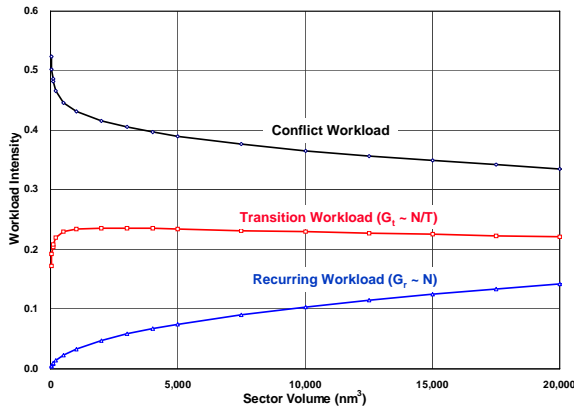


Figure 10. Variation of workload components with sector volume (4x1 rectangular sectors operating at design capacity).

When this hypothetical optimal sector operates at capacity, the conflict workload component  $G_c$  dominates for all sector volumes. (Transition workload will increase relative to conflict workload in sectors with less favorable flow.) As a sector of fixed altitude and shape becomes smaller, the available airspace drops faster than the peak traffic, causing a growth in density and thus conflict rate. The transition workload component  $G_t$  is proportional to sector capacity  $N_m$  divided by transit time  $T$ . It remains relatively invariant to volume because sector

capacity and transit time both increase approximately as the square root of sector volume. The recurring workload component  $G_r$  is proportional to sector capacity  $N_m$ . It thus increases roughly as the square root of sector volume.

### Other Capacity Models and Parameters

As noted previously, the original Schmidt model [16] included only two workload types: a routine workload component equivalent to our transition and recurring workload and a conflict component. Rather than calibrating model parameters based on sector capacity data, Schmidt used real-time controller simulations to estimate the model service times. The observed controller transition service time  $\tau_t$  for “low arrival” sectors was 46s, and  $\tau_t$  for “high transition” sectors was 28s. The controller conflict service time  $\tau_c$  was 55s for all sectors.

Figure 11 compares model design capacities for three cases: our model with service times fit to CWIS sector data, Schmidt’s low sector model, and Schmidt’s high sector model. The figure assumes sectors of fixed height and shape in which transit time varies with sector volume.

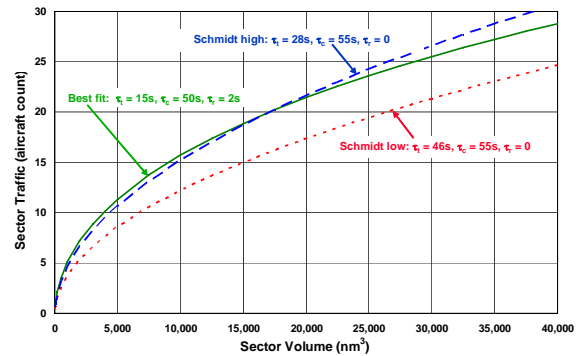


Figure 11. Design capacity comparison for 10Kft high, 4x1 rectangular sectors, from three models.

Schmidt’s high-sector result agrees closely with ours. Because he does not include an explicit recurring workload component, his result tends to overestimate capacity for larger sectors and underestimate capacity for smaller sectors.

Schmidt’s low-sector result gives significantly lower design capacity. If valid, this would imply that transition workload dominates in low sectors, whereas conflict workload dominates in high sectors. The two types of sectors would thus have different priorities for ATM task automation.

Although we have not separately analyzed low arrival sectors, we have compared the peak traffic counts of all low, high, and super-high sectors in the

CWIS domain. We observe a slightly lower capacity in low sectors that implies a transition service time of 20s (compared to 15s for high and super-high sectors). Taken alone, this 5s increase in  $\tau_t$  would not cause transition workload to dominate in low sectors. However, transition workload would be expected to dominate low sectors that are not elongated or that have significant transverse flow.

Majumdar determined the effect of vertical rates on throughput using data from the Eurocontrol RAMS simulation [12]. The Majumdar model used peak sector throughput (in units of aircraft per hour) as a measure of sector capacity for aircraft in level flight. His level-flight throughput value (derived from subjective controller estimates for a single busy European sector) was  $T = 54$  aircraft/hr/controller. Because throughput is simply the transition rate, it has the same weak dependence on sector volume that appears in the transition workload intensity curve of Figure 10. Numerical throughput values predicted by our workload model are consistent with Majumdar's value, but throughput does not account for conflicts or recurring tasks and is thus not a sufficient indicator of design capacity.

Figure 12 compares the predictions of Majumdar's constant-throughput model with the CIWS traffic data. The model does not fit the observed traffic data because its predictions depend only on sector length.

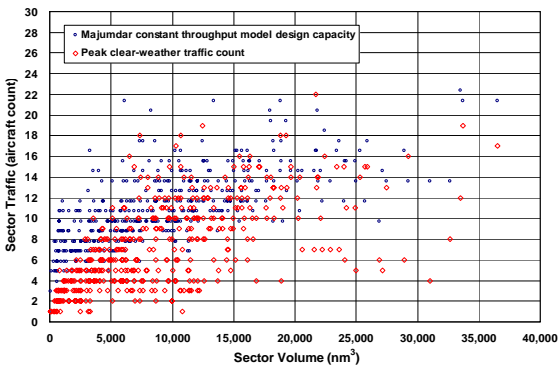


**Figure 12. Constant-throughput model design capacity compared to CIWS peak traffic counts.**

## Conclusions

A macroscopic workload model that uses operationally reasonable parameters can provide design capacity estimates that fit observed peak traffic data for a wide range of sectors shapes and volumes. The quality of the agreement is significant in view of the simple nature of the model.

The model explains important observed operational relationships such as the approximate square-root

relationship between sector capacity and volume and the relationship of capacity to sector length.

The design capacity model can be used for refining flow management alert thresholds and for guiding storm re-routing by providing individual sector capacity estimates that account for anticipated flow direction. Sector workload estimates will also help analyze the benefits of air traffic management automation, and prioritize ATM automation research by identifying manual tasks with higher workload.

## References

1. Bilimoria, Sridhar, and Chatterji, "Effects of Conflict Resolution Maneuvers and Traffic Density on Free Flight", Paper No. 96-3767, AIAA GNC Conference, San Diego, CA, 1996.
2. Donahue, "A Simplified Air Transportation System Capacity Model", Journal of ATC, April-June 1999.
3. Andrews, Welch, and Erzberger, "Safety Analysis of Advanced Separation Concepts", 6<sup>th</sup> USA-Europe ATM Seminar, Baltimore, 2005 (and ATC Quarterly, Vol. 10, No.4.)
4. Laudeman, Sheldon, Branstrom, and Brasil. "Dynamic Density: An Air Traffic Management Metric", NASA-TM-1998-112226, 1998.
5. Masalonis, Callahan, and Wanke, "Dynamic Density and Complexity Metrics for Real Time Traffic Flow Management", 5<sup>th</sup> USA-Europe ATM Seminar, Budapest, 2003.
6. Delahaye and Puechmorel, "Air Traffic Complexity: Towards Intrinsic Metrics", 3<sup>rd</sup> USA/Europe ATM Seminar, Napoli, Italy, 2000.
7. Histon, Aigoin, Delahaye, Hansman, and Puechmorel, "Introducing Structural Considerations into Complexity Metrics", 4<sup>th</sup> USA/Europe ATM Seminar, Santa Fe, NM, 2001.
8. Chatterji and Sridhar, "Measures for Air Traffic Controller Workload Prediction", 1st AIAA Aircraft Technology, Integration, and Operations Forum, Los Angeles, CA, 2001.
9. Sridhar, Sheth, and Grabbe, "Airspace Complexity and its Application in Air Traffic Management", 2<sup>nd</sup> USA/Eurocontrol ATM Seminar, Orlando Florida, 1998.
10. Weber, Evans, Wolfson, DeLaura, Moser, Martin, Welch, Andrews, and Bertsimas, "Improving Air Traffic Management during Thunderstorms", 24<sup>th</sup> DASC, Washington DC, 2005.
11. DeLaura and Allan, "Route Selection Decision Support in Convective Weather: A Case Study of the Effects of Weather and Operational Assumptions on Departure Throughput", 5<sup>th</sup> USA/Europe ATM Seminar, Budapest, Hungary, 2003.

12. Majumdar, Ochieng, and Polak, "Estimation of Capacity of European Airspace from a Model of Controller Workload", *J. Navigation*, 55, 381-403, 2002.
13. Sud, Wanke, Ball, and Carlson-Rhodes, "Air Traffic Flow Management - Collaborative Routing Coordination Tools", AIAA-2001-4112, AIAA GNC, Montreal, Canada, 2001.
14. Denery, Erzberger, Davis, Green, and McNally, "Challenges of Air Traffic Management Research: Analysis, Simulation, and Field Test", AIAA-97-3832, AIAA GNC, New Orleans, Louisiana, 1997.
15. Schmidt, "On Modeling ATC Work Load and Sector Capacity", *AIAA J. Aircraft*, Vol. 13, No. 7, 1976.
16. Schmidt, "A Queuing Analysis of the Air Traffic Controller's Work Load", *IEEE Trans. Systems, Man, Cybernetics*, Vol. SMC-8, No. 6, 1978.
17. Andrews and Welch, "Workload Implications of Free Flight Concepts", 1<sup>st</sup> USA/EUROCONTROL ATM Seminar, Saclay, France, 1997.
18. Roy, Sridhar, and Verghese, "An Aggregate Dynamic Stochastic Model for an Air Traffic System", 5<sup>th</sup> USA/Europe ATM Seminar, Budapest, Hungary, 2003.
19. Evans and Ducot "Corridor Integrated Weather System", *Lincoln Lab. J.* Vol. 16, No.1, 2006.

## Author Biographies

### *John W. Andrews*

Mr. Andrews is a senior staff member in the Surveillance Systems Group at M.I.T. Lincoln Laboratory. He was one of the senior system analysts during the development of the Traffic Alert and Collision Avoidance System and has made contributions to tracking techniques, algorithm analysis, human subject flight testing, and the modeling of pilot visual acquisition performance. He has served as a consultant to the National Transportation Traffic Board in the investigation of mid-air collisions. Mr. Andrews holds a B.S. in physics from the Georgia Institute of Technology and an S. M. in aeronautical engineering from M.I.T.

### *Brian D. Martin*

Mr. Martin is an assistant staff member of the Weather Sensing Group at M.I.T. Lincoln Laboratory. His current research includes weather-traffic flow management integration in the en route and TRACON airspace. Mr. Martin is a member of the American Meteorological Society and holds a B.S. and an M.S. in meteorology from The Florida State University.

### *Banavar Sridhar*

Dr. Sridhar worked at Systems Control, Inc., Palo Alto, CA and Lockheed Palo Alto Research Center before joining NASA Ames Research Center in 1986. At NASA, Dr. Sridhar has lead projects on the development of automation tools for rotorcraft and other vehicles. Currently, he serves as Chief, Automation Concepts Branch, managing research activities in Next Generation Air Transportation Technologies. His research interests are in the application of modeling and optimization techniques to aerospace systems. Dr. Sridhar received the 2000 IEEE Controls Systems Technology Award for his contributions to the development of modeling and simulation techniques for multi-vehicle traffic networks and advanced air traffic systems. He led the development of traffic flow management software for the Future ATM Concepts Evaluation Tool (FACET), which received the NASA Software of the Year Award in 2006. He is a Fellow of the IEEE and the AIAA. Dr. Sridhar holds a B.E. in electrical engineering from the Indian Institute of Science and an M.S. and a Ph.D. in electrical engineering from the University of Connecticut.

### *Jerry D. Welch*

Dr. Welch is a senior staff member in the Surveillance Systems Group at M.I.T. Lincoln Laboratory. He was on the team that initiated the development of the FAA's Mode S beacon system, leading the Mode S transponder design and standardization effort. He led Lincoln Laboratory's program to develop surveillance techniques for TCAS collision avoidance. He supported the FAA and NASA in the development of the Center/TRACON Automation System. His current research includes aviation system capacity analysis and decision support tool benefits analysis. Dr. Welch holds an S.B. and an S.M. in electrical engineering from M.I.T. and a Ph.D. in electrical engineering from Northeastern University.

## Acknowledgements

This work is sponsored by NASA Ames under Air Force Contract #FA8721-05-C-0002. Opinions, interpretations, recommendations, and conclusions are those of the authors and are not necessarily endorsed by the United States Government.